

A critical phenomenological study of inclusive photon production in hadronic collisions

P. Aurenche¹, M. Fontannaz², J.Ph. Guillet¹, B. Kniehl³, E. Pilon¹, M. Werlen¹

¹ Laboratoire d'Annecy-le-Vieux de Physique Théorique LAPTH, B.P. 110, F-74941 Annecy-le-Vieux Cedex, France^a

² Laboratoire de Physique Théorique et Hautes Energies LPTHE, Bât. 211, Université de Paris-Sud, F-91405 Orsay Cedex, France^b

³ Max-Planck-Institut für Physik (Werner-Heisenberg-Institut), Föhringer Ring 6, D-80805 München, Germany

Received: 23 November 1998 / Published online: 22 March 1999

Abstract. We discuss fixed target and ISR inclusive photon production and attempt a comparison between theory and experiments. The dependence of the theoretical predictions on the structure functions, and on the renormalization and factorization scales is investigated. The main result of this study is that the data cannot be simultaneously fitted with a single set of scales and structure functions. On the other hand, there is no need for an additional primordial k_T to force the agreement between QCD predictions and experiments, with the possible exception of one data set. Since the data cover almost overlapping kinematical ranges this raises the question of consistency among data sets. A comparative discussion of some possible sources of experimental uncertainties is sketched.

1 Introduction

Despite many years of intense experimental [1–10] and theoretical [11–14] efforts the inclusive production of prompt photons in hadronic collisions does not appear to be fully understood. No consensus has been reached concerning the phenomenology of these processes. An attractive possibility made use of the intrinsic ambiguities of fixed order perturbation theory to define the various unphysical scales entering the theoretical predictions by means of various “optimisation” prescriptions [15–18]: an excellent agreement [12, 19–21] between theory and experiments over the whole available range of energy and transverse momentum was thus obtained with a single set of structure functions and a unique value of A_{QCD} . More recently however it has been proposed to fix the unphysical scales at some arbitrary “physical” values and to introduce an extra non-perturbative parameter, called the “primordial transverse momentum” of the partons in the hadrons which is fitted to data at each energy [8, 22–25]. This parameter increases with energy (technically speaking it is therefore not an “intrinsic” momentum) and this is interpreted as taking into account the effects of multiple soft gluon emission associated to the hard partonic scattering.

Motivated by the recent publication of two new sets of fixed target data and using the latest up-to-date theoretic-

cal calculations we discuss the phenomenology of inclusive prompt photon production. The new data are those of the UA6 proton-proton and antiproton-proton experiment at a center-of-mass energy $\sqrt{s} = 24.3$ GeV [9] and of the E706 proton-Beryllium and pion-Beryllium experiment at $\sqrt{s} = 31.6$ GeV and at $\sqrt{s} = 38.8$ GeV [8]. To avoid further ambiguities associated to the criteria of isolation we do not discuss the colliders data on the production of isolated prompt photons.

We first set the theoretical framework by recalling the main features of the complete next-to-leading order (NLO) calculations in perturbative Quantum Chromodynamics (QCD). The intrinsic uncertainties of the NLO expressions are related to the choice of three arbitrary scales: the renormalization scale, the factorization scale associated to the initial state collinear singularities and the fragmentation scale related to the collinear fragmentation of a parton into a photon. A rather complete numerical study of these uncertainties is carried out. The main feature is that there is no stability zone in the fixed target energy range unlike what has been observed at higher energies [13]. Arbitrarily choosing the scales we show that we can get a reasonable agreement with all considered data except with the E706 [8] data obtained using nuclear targets and the older R806 data [2] from the ISR. This may raise the possibility of inconsistency among various data sets.

2 Theoretical framework and ambiguities

Because of the well-known anomalous photon component the cross section for inclusive photon production takes a

^a URA 14-36 du CNRS, associée à l'Université de Savoie

^b URA 63 du CNRS

e-mail addresses: aurenche@lapp.in2p3.fr,
fontannaz@qcd.th-u-psud.fr, guillet@lapp.in2p3.fr,
kniehl@mppmu.mpg.de, pilon@lapp.in2p3.fr,
monique.werlen@cern.ch

more complicated form than for pure hadronic reactions. The differential cross section in transverse momentum p_T and rapidity η can be written as a sum of two components:

$$\frac{d\sigma}{d\mathbf{p}_T d\eta} = \frac{d\sigma^{\text{dir}}}{d\mathbf{p}_T d\eta} + \frac{d\sigma^{\text{brem}}}{d\mathbf{p}_T d\eta} \quad (1)$$

where we have distinguished the “direct” component σ^{dir} from the “bremsstrahlung” one σ^{brem} . Each of these terms is known in the next-to-leading logarithmic approximation in QCD *i.e.* we have

$$\frac{d\sigma^{\text{dir}}}{d\mathbf{p}_T d\eta} = \sum_{i,j=q,g} \int dx_1 dx_2 F_{i/h_1}(x_1, M) F_{j/h_2}(x_2, M) \frac{\alpha_s(\mu)}{2\pi} \left(\frac{d\hat{\sigma}_{ij}}{d\mathbf{p}_T d\eta} + \frac{\alpha_s(\mu)}{2\pi} K_{ij}^{\text{dir}}(\mu, M, M_F) \right) \quad (2)$$

and

$$\frac{d\sigma^{\text{brem}}}{d\mathbf{p}_T d\eta} = \sum_{i,j,k=q,g} \int dx_1 dx_2 \frac{dz}{z^2} D_{\gamma/k}(z, M_F) F_{i/h_1}(x_1, M) F_{j/h_2}(x_2, M) \left(\frac{\alpha_s(\mu)}{2\pi} \right)^2 \left(\frac{d\hat{\sigma}_{ij}^k}{d\mathbf{p}_T d\eta} + \frac{\alpha_s(\mu)}{2\pi} K_{ij,k}^{\text{brem}}(\mu, M, M_F) \right) \quad (3)$$

where the parton densities in the initial hadrons F_{i/h_1} and F_{j/h_2} depend on the factorization scale M while the parton to photon fragmentation functions $D_{\gamma/k}$ depend on the fragmentation scale M_F . The renormalization scale μ appears in the strong coupling α_s . The higher order correction terms to the direct and bremsstrahlung cross sections, K_{ij}^{dir} [12,14] and $K_{ij,k}^{\text{brem}}$ [26] respectively, are known and we shall use their expressions in the \overline{MS} convention. The dependence of these functions on the kinematical variables $x_1, x_2, z, \sqrt{s}, p_T$ and η has not been explicitly displayed. All the quantities entering the above equations have been either calculated (K_{ij}^{dir} and $K_{ij,k}^{\text{brem}}$) or have been determined (see *e.g.* [19,27–29] for $F_{i/h}$ and [30,31] for $D_{\gamma/k}$) at the required level of accuracy by next-to-leading order fits to the data. The knowledge of $A_{\overline{MS}}$, from deep-inelastic experiments for example, completely specifies the NLO expression of the running coupling $\alpha_s(\mu)$. It is important to stress that the scales μ, M and M_F are arbitrary. The dependence in the first two scales partially compensates within each of (2) and (3) between the lowest order term and the correction term. The dependence in the fragmentation scale is more complex because of the dual nature of the photon which acts either as a parton (anomalous part) or a hadron. We come back to this point in great detail below. For our present purposes, it is enough to know that the M_F dependence of the photon fragmentation function is compensated partly by terms in K^{dir} of (2) and partly by terms in K^{brem} of (3). Since the scale M_F is arbitrary, it is clear that (2) and (3) which depend essentially monotonically on the scale M_F do not have an independent physical meaning: only the sum, (1), has a

chance to be (relatively) independent of M_F and therefore is interpreted as a physical quantity.

The fundamental ambiguity of the perturbative prediction is due to the fact that the three scales μ, M and M_F are not determined by the theory. Roughly speaking they are parameters which control how much of the higher order effects are resummed in $\alpha_s(\mu), F_{i/h}$ and $D_{\gamma/k}$ respectively and how much is treated perturbatively in K_{ij}^{dir} and $K_{ij,k}^{\text{brem}}$. In order to illustrate this problem keeping however the numerical work at a reasonable level we proceed as follows. We fix arbitrarily the fragmentation scale M_F and the factorization scale M . The remaining scale μ is then determined by solving the algebraic equation [16,18]

$$\frac{d(d\sigma/d\mathbf{p}_T d\eta)}{d\ln(\mu)} = 0. \quad (4)$$

The result is illustrated in the left picture of Fig. 1 for the inclusive production of photons in proton-beryllium reaction at $\sqrt{s} = 38.8$ GeV, $p_T = 6.12$ GeV/c. We see that at fixed M_F there is a stability point (minimum) of the cross section as M varies which is a feature of a reliable perturbative prediction. However this stability point does not go through an extremum when the fragmentation scale varies. An alternative choice for the renormalization scale μ consists in setting, for example, $\mu = M$ rather than using (4). This leads to the right hand picture in Fig. 1: again no stability is achieved in the fragmentation scale while a stable point (maximum) appears when varying $\mu = M$ at fixed $M_F^2 > 24$ GeV². Therefore, we do not have a stable point on the M, M_F sheet and one is somewhat at a loss about which scale one should choose to make predictions. This pessimism should be tempered however by noticing that there is a wide domain of relative stability for the values $M^2 < 10$ GeV² and $M_F^2 < 300$ GeV² (left picture) or $M_F^2 > 24$ GeV² where a maximum in M can be obtained (right hand picture). Despite the completely different scale variation patterns of the two pictures in Fig. 1 it should be noted that, for a given fragmentation scale, the theoretical cross section estimates at the stable points are numerically very close: they differ by less than 1%. Finally, when increasing M_F^2 from 24 GeV² to 300 GeV² the optimal predictions decrease by less than 20%. It should be reminded that at much higher energies, in the Tevatron energy range and above, a stable point could be obtained for the inclusive photon cross section [13].

To understand the reason of the present instability under variation of the fragmentation scale one can make the following observations. Consider the evolution equation of the photon fragmentation function. It is given by (dropping the longitudinal variable z and denoting instead the convolution in z by the notation \otimes)

$$\frac{dD_{\gamma/i}(M_F)}{d\ln(M_F^2)} = \mathbf{P}_{\gamma i} + \frac{\alpha_s(M_F)}{2\pi} \sum_{j=q,g} P_{ji} \otimes D_{\gamma/j} \quad (5)$$

where the $\mathbf{P}_{\gamma i}$ and P_{ji} are the appropriate Altarelli-Parisi splitting functions which admit a perturbative expansion in α_s . For consistency we keep the first two terms in our

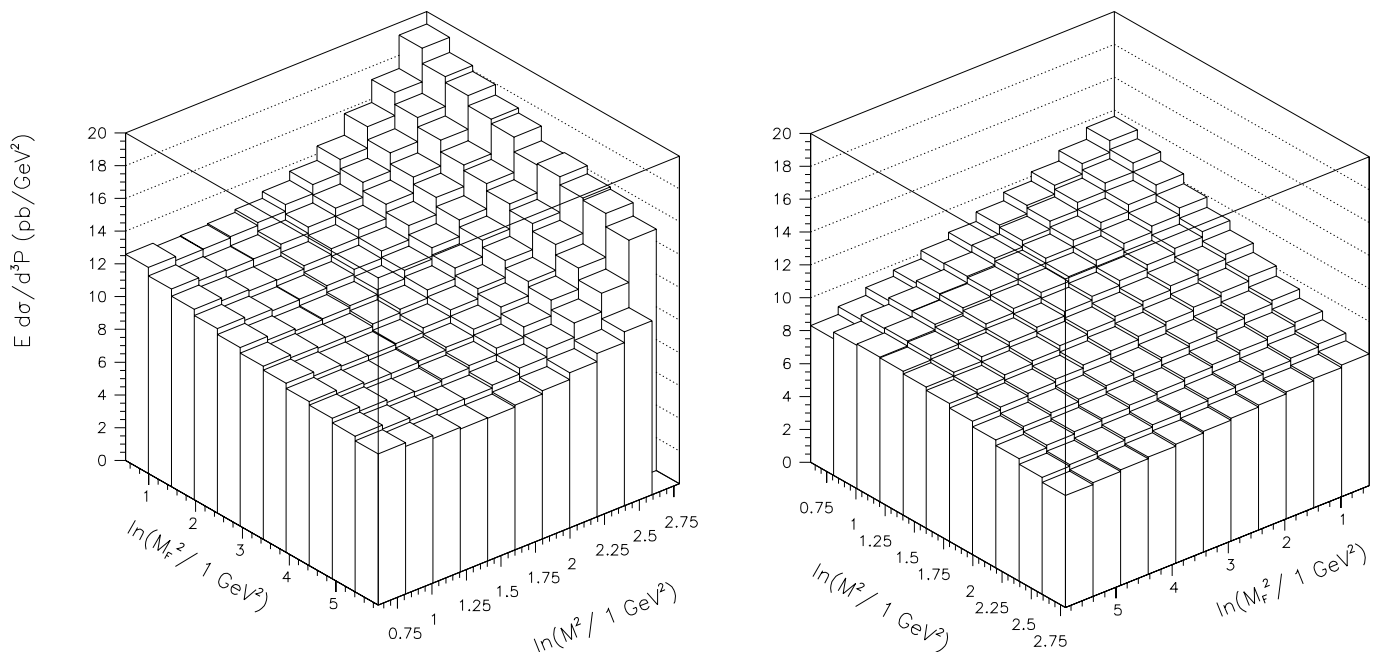


Fig. 1. Variation of the inclusive photon production cross section for proton-beryllium at $E_{\text{lab}} = 800$ GeV, $p_T = 6.12$ GeV/c, $\eta = 0.$, as a function of the factorization scale and the fragmentation scale; *left*: the renormalization scale is “optimized” according to (4); *right*: the renormalization scale is set equal to the factorization scale

analysis, namely

$$\mathbf{P}_{\gamma i} = \mathbf{P}_{\gamma i}^{(0)} + \frac{\alpha_s(M_F)}{2\pi} \mathbf{P}_{\gamma i}^{(1)} \quad (6)$$

and similarly for $P_{j i}$. The solution to (5) can be written as the sum of the anomalous part and the non-perturbative part:

$$D_{\gamma/k}(z, M_F) = D_{\gamma/k}^{AN}(z, M_F) + D_{\gamma/k}^{NP}(z, M_F). \quad (7)$$

The component $D_{\gamma/k}^{AN}(z, M_F)$ is fully calculable and it is a particular solution of the full inhomogeneous set of (5). The non-perturbative part (modeled following the Vector Meson Dominance (VMD) ideas) $D_{\gamma/k}^{NP}(z, M_F)$ obeys the usual homogeneous evolution equations of hadronic structure functions *i.e.* (5) with $\mathbf{P}_{\gamma i} = 0$. The M_F scale dependence of $D_{\gamma/k}^{NP}$, appearing in $d\sigma^{\text{brem}}$, compensates between the two terms of the right hand side of (3) as it should be for purely hadronic reactions. In contrast, the scale variation of $D_{\gamma/k}^{AN}$ associated to the inhomogeneous term $\mathbf{P}_{\gamma k}$ is compensated by a similar term in K_{ij}^{dir} of (2). It turns out that, in the kinematical region probed by fixed target experiments, such a scale compensation is not properly achieved. Indeed, due to steeply falling partonic cross sections, the average value of the variable z in the bremsstrahlung process is rather high, $z \sim .8$. In that domain, we can safely neglect the gluon fragmentation function (as well as the non-perturbative VMD input) and check that the approximation

$$D_{\gamma/q}(z, M_F) = \frac{\mathbf{c}_{\gamma q}(z)}{\alpha_s(M_F)} + \mathbf{d}_{\gamma q}(z)$$

$$\sim b \mathbf{c}_{\gamma q}(z) \ln(M_F^2/\Lambda_{\overline{MS}}^2) + \mathbf{d}_{\gamma q}(z), \quad (8)$$

with the moments ($\mathbf{c}(n) = \int_0^1 dz z^{n-1} \mathbf{c}(z)$) of the $\mathbf{c}_{\gamma q}(z)$ function given by

$$\mathbf{c}_{\gamma q}(n) = \frac{\mathbf{P}_{\gamma q}^{(0)}(n)}{b - P_{qq}^{(0)}(n)/2\pi}, \quad (9)$$

satisfy (5) (neglecting $\mathcal{O}(\alpha_s)$ terms). In the above equations the parameter b is the well known positive constant governing the evolution of the strong coupling in the leading logarithmic approximation

$$\frac{d\alpha_s(M_F)}{d\ln(M_F^2)} = -b (\alpha_s(M_F))^2 (1 + b_1 \alpha_s(M_F)). \quad (10)$$

At large z , the function $b \mathbf{c}_{\gamma q}(z)$ is much smaller than the function $\mathbf{P}_{\gamma q}^{(0)}(z)$ which appears as the coefficient of the $\ln(M_F^2)$ dependence in (2). This can be guessed from (9) since $P_{qq}^{(0)}(n)$ is negative at large n , equivalently large z , as required by the negative scaling violations of the quark fragmentation function. The relative smallness of $b \mathbf{c}_{\gamma q}(z)$ is understood by the fact that it represents the shape of the fragmentation function of the quark into a photon after multiple gluon emission while $\mathbf{P}_{\gamma q}^{(0)}(z) \sim (1 + (1-z)^2)/z$ describes the fragmentation at the lowest order level (without gluon emission). The overall scale M_F dependence of (1) is then a weighted average over large z values of the combination

$$(b \mathbf{c}_{\gamma q}(z) - \mathbf{P}_{\gamma q}^{(0)}(z)) \ln(M_F) \quad (11)$$

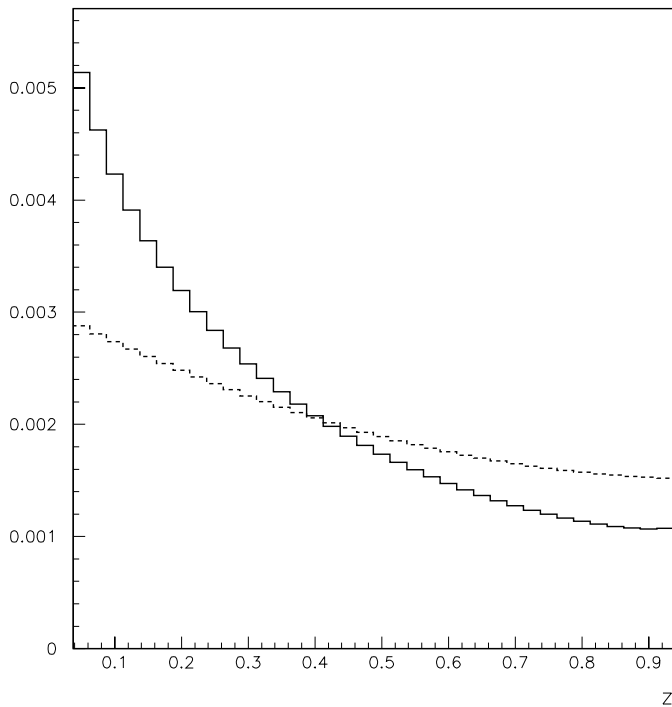


Fig. 2. *solid line:* z dependence of the perturbative component of the photon fragmentation function (8); *dashed line:* z dependence of the compensating term proportional to $\mathbf{P}_{\gamma q}^{(0)}(z)$. The scale is $M_F = 6$ GeV

which is always negative in the large z range, in agreement with the results of Fig. 1. This point is illustrated more precisely on Fig. 2 which compares, at a fixed value of M_F , the variation in z of $D_{\gamma/q}$ of (8) with that of the compensating term proportional to $\mathbf{P}_{\gamma q}$. As anticipated, the compensating term has a less steep dependence and largely dominates at large z . Since the effective value of z in inclusive photon production at E706 energies increases from $z \sim .85$ to about $z \sim .93$ when p_T varies from 5 GeV/c to 10 GeV/c it is clear that expression (11) is negative in the region of interest¹.

This discussion concentrated only on the scale variation driven by the inhomogeneous term ($\mathbf{P}_{\gamma q}$) in (5). The homogeneous term, included in our calculation, somewhat weakens the dependence in expression (11) but does not change the overall behaviour. We do not see how to overcome this basic instability of the perturbative prediction for the inclusive production of direct photon in hadronic collisions. Notice that the perturbative approach is not spoiled by the presence of large $\ln(1-z)$ terms, for they cancel each other (at order α_s^2) between the direct contribution (2) and the bremsstrahlung contribution (3) [31]. Recently, two groups [32] have studied, in hadronic processes, the resummation of collinear and soft logarithms which become large in the limit where x_1 and x_2 are close to 1. Although the average values of x_1 and x_2 in (2,3)

¹ As p_T increases the relative importance of the fragmentation terms decreases compared to direct photon production terms

are of the order of x_T , the resummed expressions might slightly change the values of the predictions obtained in this paper. The stability with respect to the scales μ and M could also be improved. These types of corrections are not considered here. It would be interesting to investigate their impact on the prompt photon phenomenology.

We propose to bracket the theoretical results by choosing two extreme values of the fragmentation scale. Let us note that making the choice $M_F = \mu$ may accidentally reduce the overall scale dependence of the cross section since, for example, one power of $\alpha_s(\mu)$ in (3) is compensated by the $1/\alpha_s(\mu)$ factor of $D_{\gamma/q}$. We do not advocate this choice although we will often use it for practical reasons in the following.

Before closing these theoretical preliminaries, let us make a technical comment. It concerns the definition of $\alpha_s(\mu)$. The solution of the NLO evolution equation of the coupling (10) leads to the following relation in the \overline{MS} scheme

$$b \ln(\mu^2/\Lambda_{\overline{MS}}^2) = \frac{1}{\alpha_s(\mu)} + b_1 \ln\left(\frac{b \alpha_s(\mu)}{1 + b_1 \alpha_s(\mu)}\right), \quad (12)$$

where

$$b = \frac{(33 - 2N_f)}{12\pi} \quad \text{and} \quad b_1 = \frac{(153 - 192N_f)}{2\pi(33 - 2N_f)}, \quad (13)$$

with $N_f = 4$, the number of flavors. To obtain $\alpha_s(\mu)$ explicitly one may invert exactly (numerically) this equation, or one may invert it approximately (analytically) keeping the first two terms in the expansion of $\alpha_s(\mu)$ in terms of $1/\ln(\mu^2/\Lambda_{\overline{MS}}^2)$. In the region of interest for this study the difference between the obtained values of $\alpha_s(\mu)$ for a given μ may reach 5%. We advocate, and we will use in the following, the “exact” estimate of $\alpha_s(\mu)$.

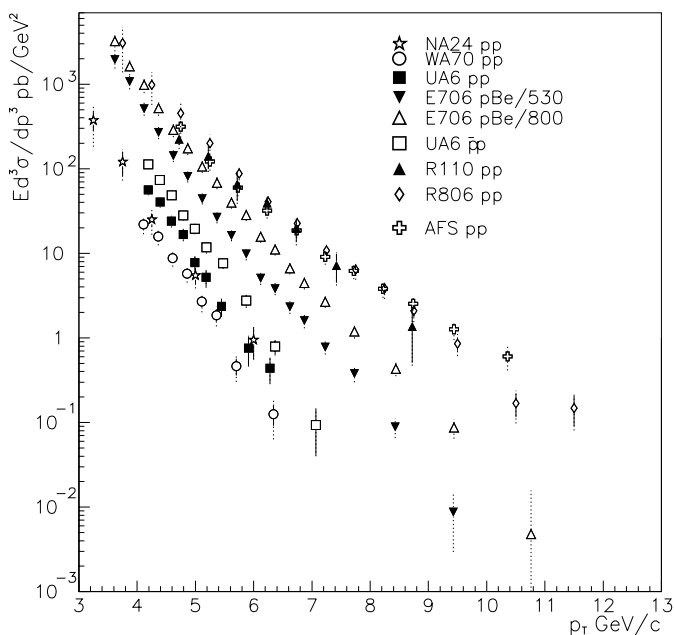
3 Phenomenology of prompt photon production

Let us first summarize the data sets used in the following discussion. This is done in Table 1. To avoid uncertainties due to the pion structure functions we restrict our discussion to the case of proton induced reactions. Concerning E706 and the possible nuclear effects on the parton distributions in the Beryllium target we follow the same prescription as the collaboration and adjust the theoretical predictions with the factor $A^{\alpha-1}$ with $\alpha = 1.04$. In this way the resulting cross section is normalized per nucleon.

The inclusive differential cross sections are shown in Fig. 3 where they are plotted as a function of p_T . Already, we anticipate some difficulties when comparing the data sets: for example, the relatively large difference between the WA70 and UA6 cross sections at low p_T cannot be accounted for by the small \sqrt{s} change between experiments nor by the different rapidity coverage; one also observes almost an order of magnitude difference between the UA6(pp) data and the E706(530 GeV) for an energy change from $\sqrt{s} = 24$ GeV to $\sqrt{s} = 31.6$ GeV while the

Table 1. Summary of the main features of the data sets. The transverse and longitudinal variables x_T , x_F are defined by $x_T = 2p_T/\sqrt{s}$ and $x_F = 2p_L/\sqrt{s}$

Collaboration	Reaction	\sqrt{s} [GeV]	p_T range [GeV/c]	x_F /rapidity range	x_T range
WA70[3]	$p p$	23.0	$p_T > 4.0$	$-.35 < x_F < .45$	$x_T > .35$
UA6[9]	$p p$	24.3	$p_T > 4.1$	$-0.1 < \eta < 0.9$	$x_T > .34$
UA6[9]	$\bar{p} p$	24.3	$p_T > 4.1$	$-0.1 < \eta < 0.9$	$x_T > .34$
E706[8]	$p Be$	31.6	$p_T > 3.5$	$-.75 < \eta < .75$	$x_T > .22$
E706[8]	$p Be$	38.8	$p_T > 3.5$	$-1.0 < \eta < 0.5$	$x_T > .18$
R806[2]	$p p$	63.	$p_T > 3.5$	$-0.2 < \eta < 0.2$	$x_T > .11$
R110[5]	$p p$	63.	$p_T > 4.5$	$-0.8 < \eta < 0.8$	$x_T > .14$
AFS/R807[6]	$p p$	63.	$p_T > 4.5$	$-0.7 < \eta < 0.7$	$x_T > .14$


Fig. 3. The differential inclusive photon cross sections as a function of transverse momentum. The cross sections are averaged over the x_F /rapidity ranges shown in Table 1. Data from the NA24 collaboration [1] are averaged in the rapidity range $-.65 < \eta < .52$

E706(800 GeV) and R806 data at low p_T have almost the same size despite an energy increase from $\sqrt{s} = 38.8$ GeV to $\sqrt{s} = 63$. GeV.

In the numerical calculations we will use several sets of recent next-to-leading order structure functions in the \overline{MS} convention. CTEQ [27] and MRS [28] will be our main sets. However, in order to compare the present results with the “old” fits done using the WA70 data we will also make use of the original ABFOW [19] sets ². Concerning the higher order calculations they have been performed using

² In our previous phenomenological studies [12, 19] the higher order calculations to the bremsstrahlung cross section were not available and a stability in the fragmentation scale could not be expected. That scale was then chosen to be \hat{s}

four light flavors and therefore $m_{\text{charm}} = 0$ in the partonic cross sections and the higher order terms. However the threshold effects due to the charm quark mass are taken into account in the fragmentation function $D_{\gamma/c}$ in such a way that at a scale $M_F \sim m_{\text{charm}}$ one recovers all the correct logarithmic factors of the exact massive calculation [31]. The most recent parametrization of the NLO parton to photon fragmentation functions of [31] will be used. In this work, two parametrizations of the fragmentation functions $D_{\gamma/i}$, based on fits to e^+e^- data, are given: we use set II parametrization which corresponds to the large non-perturbative gluon input. In fact, little difference is observed in inclusive photon production in hadronic collisions between set I and set II predictions since, as discussed in the previous section, the effective fragmentation variable z is large and the fragmentation functions are then dominated by their perturbative components.

We first discuss the comparison between theory and experiments for proton-proton and proton-antiproton (when applicable) collisions, using a fixed common scale $\mu = M = M_F$. Then we shall relax this constraint and study optimised predictions in the μ and M scales for a range of fragmentation scale in order to propose an estimate of the errors on the perturbative predictions. In the theoretical predictions we always include the NLO corrections to both the direct component and to the bremsstrahlung component (denoted ACFGF in the figures).

In order to normalize our present results to the previous ones appropriate to WA70 data we start our analysis using the ABFOW parametrization ($\Lambda_{\overline{MS}} = 230$ MeV, $x G(x, Q_0^2 = 2 \text{ GeV}^2) = (1 - x)^4$). We get with all scales in the problem set equal to $p_T/2$ a good approximation of the old optimised results and also a good agreement with the WA70 data ($\chi^2 = 8.2$ for 7 points using statistical errors only³). Comparing with the new UA6 measurements, there is an excellent agreement with the data (see Fig. 4) on the difference $\bar{p}p - pp$ (which is insensitive to the gluon density in the proton and to the parton fragmentation functions into a photon) while the $\bar{p}p$ data tend to be higher than the theory by roughly 20% and the pp data by

³ As in [19], the lowest p_T point is not included in the χ^2 evaluation, due to important systematic errors

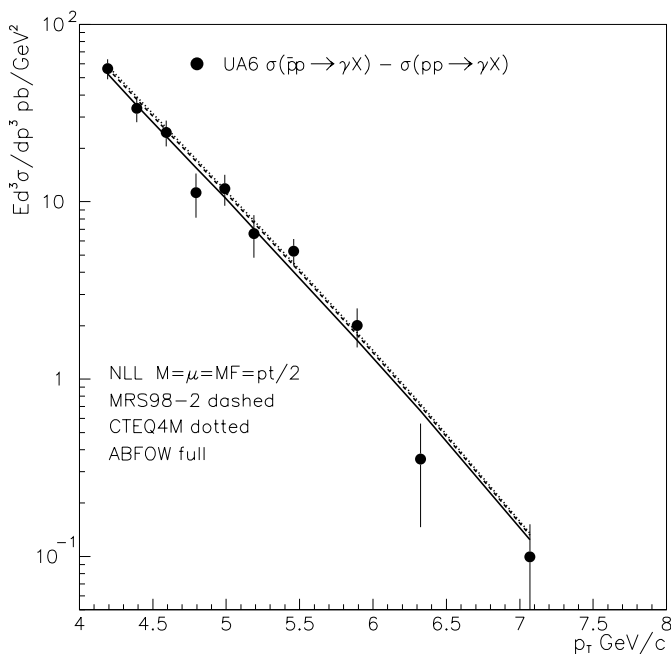


Fig. 4. Comparison of the UA6 $\bar{p}p - pp$ data [9] with the NLO theory for various sets of structure functions using the common scale $\mu = M = M_F = p_T/2$. Only statistical errors are shown

almost a factor 2 for $x_T < 0.4$ ($\chi^2 = 64.4/9$). The normalized ratios $data/theory$ are shown in Fig. 5. At large x_T the WA70 and UA6 data are mutually compatible within the error bars while there may be some relative normalization problem for the points below $x_T = 0.4$. Turning now to the ISR results one notices that they are located at small x_T values and that, for the R110 and AFS/R807 data, the ratio $data/theory$ is flat as a function of x_T ; furthermore it is compatible with 1 ($\chi^2 = 6.8/7$ for R110 and $\chi^2 = 13.7/11$ for AFS/R807⁴). In contrast, the R806 data show a marked decrease from 1.5 to 0.5 as x_T increases. It is clear that the problem of the R806 data is not related so much to the overall normalization as to the slope of the x_T distribution. In fact, it was noted before that the p_T dependence of the R806 data was incompatible with the slope of the other direct photon experiments. Besides, it was not possible to obtain a good fit simultaneously to the deep-inelastic data and to the R806 data [19]. However all ISR sets, up to $x_T = 0.3$ are point to point compatible taking into account statistical as well as systematic error bars.

The main surprise comes when comparing the E706 data to theory: at both energies we observe that the experimental points are 2 to 3 times larger than the theoretical predictions at high x_T and the ratio experiment/theory keeps increasing up to a value of 5 as x_T decreases. This had already been stressed by the E706 collaboration [8].

⁴ All the above χ^2 values are obtained using statistical errors only except in the case of AFS/R807 where only the sum of statistical errors and systematic errors added in quadrature is available

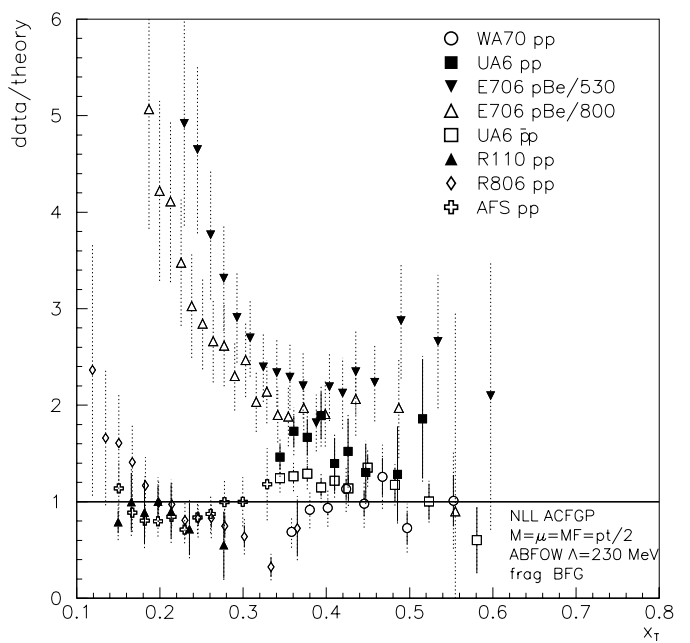


Fig. 5. Comparison of data with theory, normalized to the theoretical results, for the various experiments as a function of x_T . The ABFOW structure functions are used and all scales are set equal to $p_T/2$. Statistical error bars are shown as full lines while systematic uncertainties are added in quadrature and shown as dotted lines. An extra 5% uncertainty on the energy scale is not plotted for R110; for AFS and E706 data, statistical and systematic errors are shown combined in quadrature only

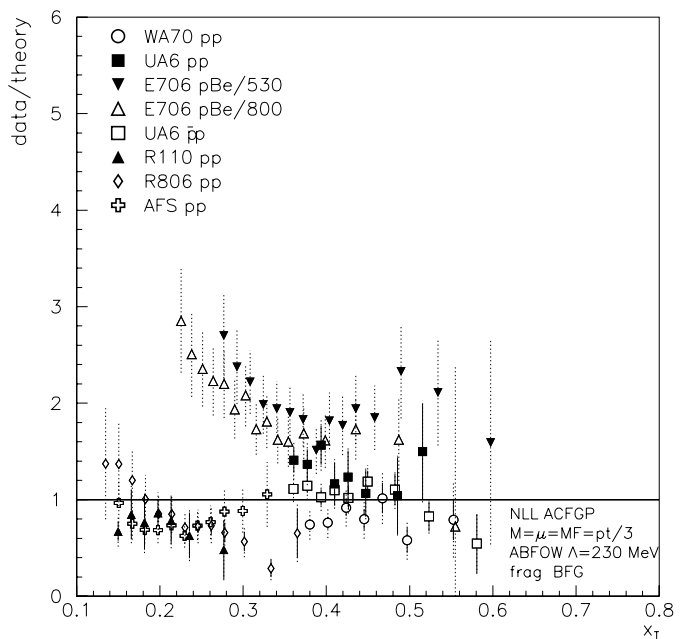


Fig. 6. Comparison of data with theory, normalized to the theoretical results, for the various experiments as a function of x_T . The ABFOW structure functions are used and all scales are set equal to $p_T/3$. Data points at scales such that $(p_T/3)^2 < Q_0^2 = 2 \text{ GeV}^2$ are not included, which explains why the points at lower x_T values in some experiments are not displayed. See Fig. 5 for further comments

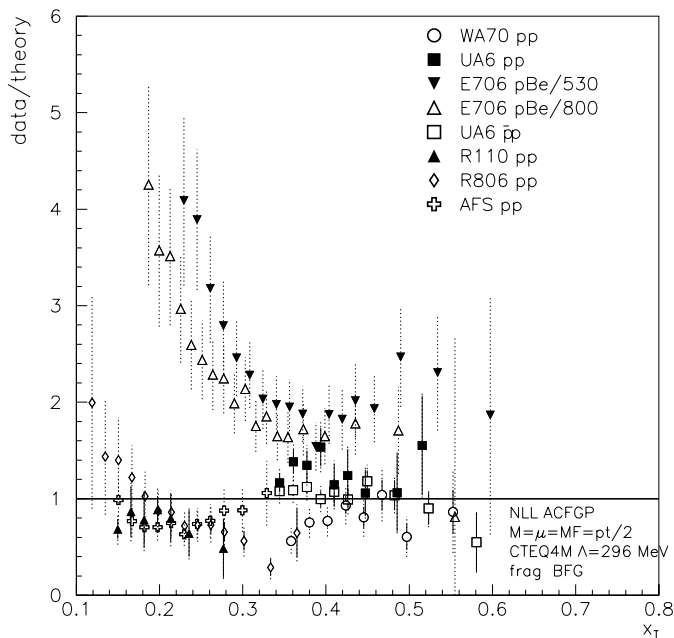


Fig. 7. Dependence in x_T of the experimental cross sections normalized to theoretical predictions using the CTEQ4M distributions. All scales in the calculations have been set to $p_T/2$ and only data points satisfying the condition $(p_T/2)^2 > Q_0^2 = 2.56 \text{ GeV}^2$ are kept. See Fig. 5 for further comments

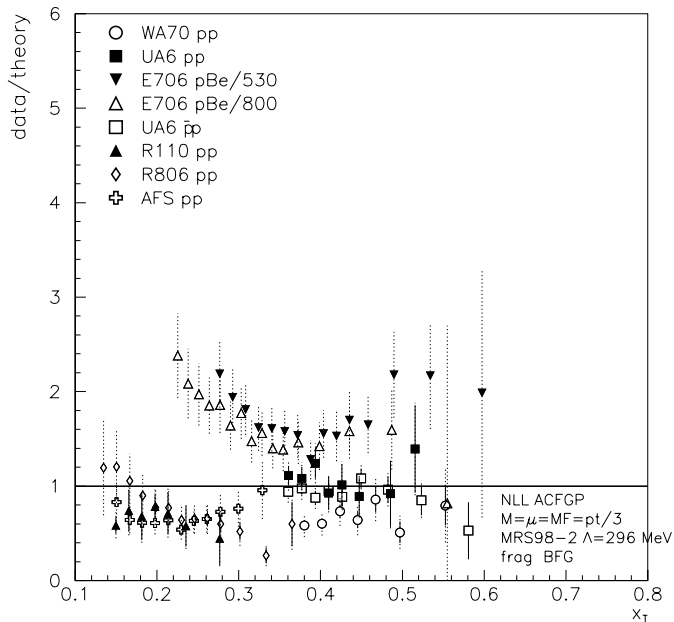


Fig. 8. Dependence in x_T of the experimental cross sections normalized to theoretical predictions using the MRS-98-2 distributions. All scales in the calculation have been set to $p_T/3$ and only data points satisfying $(p_T/3)^2 > Q_0^2 = 2. \text{ GeV}^2$ are shown. The condition $p_T > 5. \text{ GeV}/c$ (see Sect. 4) translates into $x_T > .32$ for E706 (530 GeV) and $x_T > .26$ for E706 (800 GeV) and $x_T > .16$ for ISR data. See Fig. 5 for further comments

A similar study can be conducted with the common scale in the calculation set equal to $p_T/3$ instead of $p_T/2$. The corresponding results are displayed in Fig. 6. Good agreement is achieved for the difference $\bar{p}p - pp$ and the UA6 $\bar{p}p$ data ($\chi^2 = 14.7/9$). Agreement between theory and experiment is much improved in the case the UA6 pp data ($\chi^2 = 23.1/8$) while, on the contrary, the comparison between WA70, R110 and AFS/R807 is not so satisfactory (all χ^2 values are roughly multiplied by a factor 3 compared to the analysis with scales $p_T/2$). In fact, all these data sets fall somewhat below the theoretical predictions. Concerning E706, essentially the same situation as before prevails since the theoretical predictions are rather stable (they increase by about 20 %) when changing the common scale from $p_T/2$ to $p_T/3$, namely the theory still underestimates the data by roughly a factor 2 at large x_T and much more at small x_T .

The provisional conclusion to be drawn is that there is room for a minor incompatibility in the normalization of the UA6 and WA70 pp data at low p_T while they are in perfect agreement at large transverse momentum, or to put it differently, there may be some incompatibility in the p_T dependence of the two sets of data. The ISR data are also compatible with WA70/UA6 while the E706 results stand much above all other experiments. It is to be noted that the UA6 $\bar{p}p$ data are in good agreement with the theoretical predictions both in shape and normalization.

We repeat our numerical exercises using CTEQ4A1, CTEQ4M and MRS-98 structure functions. In the case of CTEQ4A1 we obtain very much the same phenomenology as before. As illustrations, we show the comparison between data and theory using CTEQ4M with all scales equal to $p_T/2$ in Fig. 7⁵ and using MRS-98-2 with all scales equal to $p_T/3$ in Fig. 8. Figure 7 looks very similar to the case of ABFOW with the smaller common scale $p_T/3$: this is understood because of the larger value of $\Lambda_{\overline{MS}} = 296 \text{ MeV}$ for CTEQ4M (instead of 230 MeV) which yields a larger value of α_s for a given scale and therefore larger theoretical predictions. The same comment would apply to the results based on MRS-98-2 with the common scale $p_T/2$. From Fig. 8, there appears a perfect agreement between theory and the UA6 pp and $\bar{p}p$ data (the χ^2 values are 3.12/8 and 5.5/9 respectively) and a tendency to reduce the disagreement with E706 to an overall normalization factor of roughly 50 % at the cost of overestimating the ISR data and the low p_T WA70 data. Let us remark that the overall improved agreement between theory and experiment is, in part, due to dropping a few experimental points at low p_T because of the scale limitation.

It appears difficult to reconcile the E706 data with the other fixed target data: clearly their normalization is higher. At large x_T values ($x_T > .3$), one can roughly estimate from the previous figures that, when normalized to any perturbative NLO predictions, they are above the other data sets by a factor ranging from at least 50% (com-

⁵ The difference on the ratios $data/theory$ observed for the E706 points, at low p_T , between Fig. 7 and Fig. 14 of [8] arises partly because in the latter work the higher order terms in (3) were not taken into account

pared to UA6, all scales $p_T/3$) to 2.0 (compared to WA70, all scales $p_T/2$).

A further striking fact, which is obvious on all figures, is the rise of the E706 cross sections compared to the theory as x_T decreases below 0.25. We point out here that this rise is not systematic as claimed in [22]. In fact, it is not observed at all on the R110 and AFS/R807 data and it is rather weak on the R806 data which cover a lower x_T range than E706. Such a conclusion was also reached by the authors of [20]⁶.

In conclusion, no set of structure functions is able to accommodate the recent E706 data despite allowing a reasonable variation in the choice of scales. In contrast, the NLO calculations are in agreement (within the rather large experimental and theoretical error bars) with the other data sets which bracket the E706 data in energy and which, taken together, cover the large x_T range of E706.

4 Further phenomenological considerations

In order to bring their data in agreement with theory the E706 collaboration advocates the use of an extra parameter identified as a measure of the transverse momentum fluctuations of the colliding partons [33]⁷. In the present phenomenological implementation of this effect both the normalization and the shape of the p_T spectrum are affected so that the E706 collaboration is able to reproduce their data with k_T values in the range 1.2-1.3 GeV/c. For UA6 the choice $k_T = 0.7$ GeV/c gives a good agreement with the data [24]. From these values one would expect $k_T > 1.5$ GeV/c to be appropriate for ISR data which would destroy the rough agreement between data and theory displayed in the figures. From this we conclude that, including k_T effects may help some data sets (E706) to agree with theoretical predictions but it simultaneously destroys the agreement with other data sets (WA70, ISR) with theory [34]. Globally the phenomenology of "low" energy photon production is not improved, on the contrary! More precisely, except for the E706 data there is no need for an extra parameter to obtain agreement between data and theory.

Some more comments can be added concerning " k_T " smearing effects. There is no definite theoretical method to parameterize such effects and as a result different groups obtain rather different shifts of the differential cross sections, specially at low values of p_T , as it has been briefly discussed in [24]. Besides, the fitted value of " k_T " depends on the estimates used for the perturbative cross sections. In the low p_T region, the perturbative predictions become notoriously unstable because no optimum in the factorization and renormalization scales is achieved. Therefore one observes large variations in the perturbative estimates

⁶ In [20] (see also [21]) a better theoretical input than in [22], in particular a complete NLO treatment of the bremsstrahlung component, was used

⁷ In practice, more than one parameter is needed to model this effect [22]

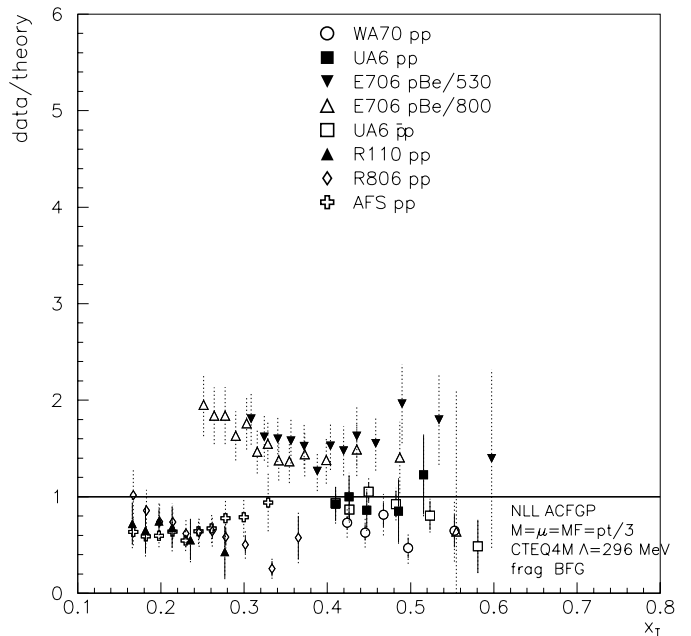


Fig. 9. Dependence in x_T of the experimental cross sections normalized to theoretical predictions using the CTEQ4M distributions. All scales in the calculations have been set to $p_T/3$ and small p_T points have been dropped as explained in the text

under changes of scales. Finally the k_T effect "observed" in single inclusive cross sections cannot be related in a direct way to the k_T effect "observed" in double inclusive cross sections (like a diphoton cross section). Indeed, the kinematical constraints are quite different in both cross sections and the perturbative soft gluons emitted prior to the hard scattering lead to very different effects for the single and for the double inclusive cross sections: for example, the "large double-logarithm" terms, $\ln^2(s/q_T^2)$ which affect the q_T spectrum of a pair, do not exist in the single inclusive cross section.

Let us now comment in some detail the agreement between QCD predictions and data. We have checked in numerical studies similar to those leading to Fig. 1 that no stable point, at fixed fragmentation scale, can be obtained for E706 at 800 GeV and $p_T < 5$. GeV/c, for example. The three-dimensional plots show a monotonic variation under changes of scales as would be obtained in a leading logarithmic calculation. We would like to interpret this fact as an indication that perturbation theory is not valid in that range since variation of the arbitrary scales leads to large variation in the predictions. For quantitative comparison between theory and experiments such points should not be included. This phenomenon occurs for the WA70/UA6 data for p_T values below 4.2 GeV/c. Let us note that at these larger values of transverse momentum the perturbative predictions are stable against moderate k_T effects ($\langle k_T \rangle < 0.4$ GeV/c). If we accept this reasonable limitation the disagreement between data sets and the theoretical predictions resides essentially in an overall normal-

Table 2. Table of χ^2 values normalized to the number of experimental points. The statistical errors and systematic errors added in quadrature are used in the evaluation of χ^2 values. Data points at scales lower than Q_0^2 are not included, which explains why the number of considered experimental points is smaller for the scale $p_T/3$ than for the scale $p_T/2$. $Q_0^2 = 2.56 \text{ GeV}^2$ for CTEQ4M and $Q_0^2 = 2. \text{ GeV}^2$ for MRS-98-2. Only the experimental points with $p_T > 4.2 \text{ GeV}/c$ for WA70/UA6 and with $p_T > 5. \text{ GeV}/c$ for ISR are kept. For R110 a 5% uncertainty on the energy scale is not included in the systematic errors

Collaboration	Reaction	\sqrt{s} [GeV]	CTEQ4M	CTEQ4M	MRS-98-2	MRS-98-2
			$\chi_{p_T/2}^2$ (stat.+syst.)	$\chi_{p_T/3}^2$ (stat.+syst.)	$\chi_{p_T/2}^2$ (stat.+syst.)	$\chi_{p_T/3}^2$ (stat.+syst.)
WA70 [3]	$p p$	23.	9.1/7	21./5	5.7/7	37.6/7
UA6 [9]	$p p$	24.3	13.7/9	2.34/6	19.0/9	3.12/8
UA6 [9]	$\bar{p} p$	24.3	5.2/10	7.45/7	6.44/10	5.51/9
R806[2]	$p p$	63.	55.4/11	91.6/11	44.9/11	80.1/11
R110[5]	$p p$	63.	5.7/6	14.1/6	3.9/6	11.2/6
AFS/R807[6]	$p p$	63.	27.8/10	71.9/10	18.2/10	71.6/10

ization factor and not in the shape of the x_T distributions as seen in Fig. 8 and Fig. 9.

To gauge the agreement between theory and experiment more quantitatively and in order to roughly take into account the systematic uncertainties we proceed in the following way. First, we calculate for each experiment the χ^2 value per number of experimental points using the statistical and systematic errors added in quadrature. The results are shown in Table 2 except for the E706 data for which the systematic errors are not yet tabulated. Both sets of structure functions (CTEQ4M and MRS-98-2) lead essentially to the same conclusions: no agreement with R806 but satisfactory agreement with the other experiments. More precisely, the UA6 $\bar{p}p$ data are in excellent agreement with both sets of structure functions, independently of the scale choice which makes them a very good channel to extract the value of $\Lambda_{\overline{MS}}$ [35]. The UA6 pp data coincide very well with both sets of predictions based on the scale choice $p_T/3$ while clearly the other experiments prefer the larger scale $p_T/2$ or even a larger scale (alternatively, a lower $\Lambda_{\overline{MS}}$ value would fit the WA70, R110 and AFS/R807 data very well as can be seen from Fig. 5). Turning now to the E706 data the ratio *data/theory* is essentially flat in the x_T region considered as perturbatively reliable (see Figs. 8 and 9) but the data are in excess of the theoretical prediction by at least 50% both at 530 GeV and 800 GeV. To summarize, it could be said that all the data sets considered could be made consistent with each other (and with the theory) if one would allow for rather large relative overall normalization shifts.

In Table 3 we show the result of such a study and give the χ^2 values based on statistical errors but fitting an overall normalization factor for each experiment. Clearly, one gets for all experiments (except R806) very good χ^2 values at the expense of sometimes unusually large factors λ . An interesting case is E706: at 530 GeV the small

χ^2 values could have been anticipated from the figures while at 800 GeV the rather large values displayed in the table are clearly due to the data points at low x_T with small statistical errors (much smaller than the systematic uncertainties). Obviously our naive procedure cannot handle such effects correctly. It would be worthwhile, in this respect, to analyse all data including the point to point as well as the overall systematic errors properly. We can just conclude from Table 3 that the price of obtaining consistency among all experimental results as well as a good agreement between theory and experiments is to allow normalization shifts in the data which are sometimes well in excess of the allowed ranges estimated from adding the different systematic errors in quadrature. It would appear that CTEQ4M, with the common scale in the theoretical predictions set equal to $p_T/3$, leads to the best phenomenology in the sense that the normalization factors λ are closest to 1, still keeping small χ^2 values. However, because of the smaller number of experimental points kept in the analysis it is not possible to argue decisively in favor of this set rather than MRS-98-2.

It was mentioned above that the shape of the E706 data at 800 GeV was not in agreement with the theory at small x_T . This raises the question of how changes of scales affect the shape of the predictions. This is studied in Fig. 10 where the theoretical results for various choices are compared to the reference case with $\mu = M = M_F = p_T/2$. Two extreme cases are considered, $M_F^2 = 2 \text{ GeV}^2$ and $M_F^2 = 300 \text{ GeV}^2$, the other scales being optimised in the sense of (4). The effect of changing the scales consists essentially in an overall shift in normalization but the increase in the cross section associated to the small M_F scale is not enough to bring the theory and the E706 data in agreement. A relative enhancement is obtained at small x_T with the (extreme) choice $M_F^2 = 2 \text{ GeV}^2$ but it is not sufficient to account for the shape of the E706/800 GeV data at low x_T . A smaller spread in the theoretical re-

Table 3. Table of χ^2 values normalized to the number of experimental points. The statistical errors are used in the evaluation of χ^2 values but, for each experiment, an overall normalization factor is allowed to vary. Only points with $p_T > 4.2$ GeV/c for WA70/UA6 and with $p_T > 5$. GeV/c for E706/ISR are kept. Strictly speaking, λ should set to 1 for AFS/R807 since the quoted errors include the systematics

Collaboration	Reaction	\sqrt{s} [GeV]	CTEQ4M	CTEQ4M	MRS-98-2	MRS-98-2
			$\chi^2_{p_T/2}$ (stat.) normaliz.	$\chi^2_{p_T/3}$ (stat.) normaliz.	$\chi^2_{p_T/2}$ (stat.) normaliz.	$\chi^2_{p_T/3}$ (stat.) normaliz.
WA70 [3]	$p p$	23.	7.55/7 $\lambda=1.46$	5.88/5 $\lambda=1.27$	9.1/7 $\lambda=1.21$	8.7/7 $\lambda=1.61$
UA6 [9]	$p p$	24.3	5.55/9 $\lambda=0.79$	3.4/6 $\lambda=0.98$	5.3/9 $\lambda=0.74$	3.5/8 $\lambda=0.93$
UA6 [9]	$\bar{p} p$	24.3	6.8/10 $\lambda=0.94$	5.5/7 $\lambda=1.11$	5.9/10 $\lambda=0.91$	5.5/9 $\lambda=1.06$
E706 [8]	$p Be$	31.6	15.7/13 $\lambda=0.52$	12.9/13 $\lambda=0.64$	17.8/13 $\lambda=0.50$	15.1/13 $\lambda=0.64$
E706[8]	$p Be$	38.8	64/13 $\lambda=0.50$	51.9/13 $\lambda=0.61$	59.7/13 $\lambda=.48$	48.7/13 $\lambda=0.60$
R806[2]	$p p$	63.	329/11 $\lambda=0.99$	278/11 $\lambda=1.17$	348/11 $\lambda=0.93$	281/11 $\lambda=1.12$
R110[5]	$p p$	63.	1.91/6 $\lambda=1.26$	1.62/6 $\lambda=1.50$	1.88/6 $\lambda=1.19$	1.61/6 $\lambda=1.43$
AFS/R807[6]	$p p$	63.	2.6/10 $\lambda=1.35$	3.2/10 $\lambda=1.58$	2.6/10 $\lambda=1.28$	2.7/10 $\lambda=1.58$

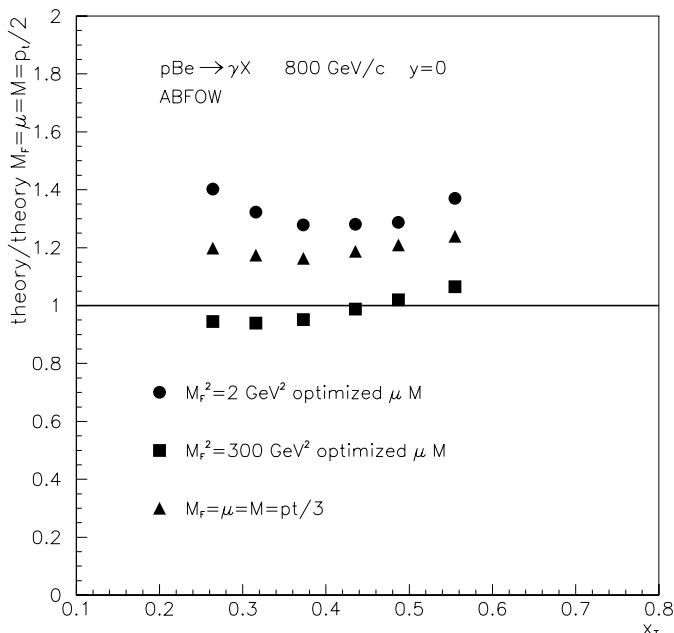


Fig. 10. Study of the sensitivity of the cross section to changes of scales for E706 at 800 GeV. All results are normalized to the cross section calculated using $\mu = M = M_F = p_T/2$

sults would, of course, be obtained had we used M_F scales proportional to p_T .

A final comment concerning the reliability of the theoretical predictions is related to the uncertainty in the behaviour of the quark distributions at large x . Recently, it has been pointed out that nuclear effects in the extraction of the quark distributions from deep-inelastic data on Deuterium had not been fully taken into account [36]. Taking these effects into account leads to a much larger d/u ratio at $x > 0.5$, increasing with x . As a consequence, the predictions for some prompt photon production rates could be affected. In fact, pp reactions should not be modified because the photon production rate is dominated by Compton-like scattering and therefore it involves the same combination of quark distributions as probed in deep-inelastic scattering on a proton, namely $(4u + d)$, which is of course not sensitive to the effects discussed in [36]. Such is not the case for nuclear targets. For pN scattering, where N is an isoscalar nucleus, $\sigma^{pN} \sim 5(u+d)$ and an increase δd in the d quark distribution manifests itself by an increase $\delta\sigma^{pN} \sim 15\delta d/4$ where the constraint $\delta u \sim -\delta d/4$ has been used. In [36] the effect of nuclear binding is parametrized as an increase of $\delta(d/u) \simeq (.1 \pm .001)(1+x)x$ of the d/u ratio. This translates into an increase of the theoretical predictions for pN cross sections

$$\frac{\delta\sigma^{pN}}{\sigma^{pN}} \sim \frac{3}{4} \delta\left(\frac{d}{u}\right) \left(1 - \frac{5}{4} \frac{d}{u}\right) \quad (14)$$

which could be as large as 20% when the relevant $\langle x \rangle$ is large enough. This is a very rough discussion since, if nuclear effects have to be disentangled when extracting the d distribution in deep-inelastic experiments they should be included (back) when making predictions for prompt photon production on (different) nuclear targets! This point certainly deserves further detailed studies.

The predictions for $\bar{p}p$ could also be modified due to the important contribution of the annihilation channel $q\bar{q} \rightarrow \gamma G$ specially at large p_T where the increase in the d/u ratio should lead to a slight decrease of the cross section (a quick estimate leads to $\delta\sigma^{\bar{p}p}/\sigma^{\bar{p}p}|_{ann} \sim -\delta(d/u)/2$ for a large enough p_T).

For lack of parton distributions incorporating this effect we do not pursue a quantitative study of this problem.

5 Experimental data sets

In view of possible incompatibilities between various data sets, let us review some specific features of the experiments. Details on systematic uncertainties are not always available. For the latest E706 data, details on energy scale uncertainty are available. For other issues, we comment on the early data analysis [7] which may not apply for the large statistical sample. It would be interesting to have such information on the large statistical sample for a detailed comparison between data sets.

5.1 Hydrogen or heavier nuclei

In fixed target experiments, the data mainly have been taken at CERN with hydrogen (with the exception of NA3 data on isoscalar Carbon target) while the published direct photon cross sections with heavier nuclei come mainly from the E706 collaboration [7, 8]. A detailed study of the nuclear corrections is in preparation [37].

5.2 Isolation criteria

All the comparisons with theory have assumed fully inclusive photon production. In fact, the prompt photon samples are always obtained with some isolation criteria, at least to remove electrons and charged hadrons in the sample. These cuts depend on the granularity of the detectors which is an important ingredient of the shower reconstruction algorithms. The data presented are usually corrected for this inefficiency.

These cuts were sizable for the pioneering ISR experiments. In the R110 sample, where the cuts were no charged tracks within 25 cm of the shower and no additional electromagnetic shower within 20 cm of the candidate photon, no correction was applied and the data are presented as biased against bremsstrahlung [5]. A proper theoretical treatment of such cuts is not available. The

R806 [2] and AFS/R807 [6] data, on the other hand, are corrected for such effects. The correction is 1.15 to 1.25 for the later but no details are given on the p_T dependence of the correction. Part of the observed discrepancies between the ISR experiments at low p_T could be attributed to this effect.

For fixed target data, two kinds of cuts are applied, one on a charged track extrapolating to the shower of the photon candidate to remove electrons and charged hadron showers, and one on the longitudinal energy deposition to remove hadronic showers in the sample. For WA70 and UA6, the cut is no charged track extrapolating within 5 cm, respectively 1.5 cm, of the shower center. For E706, no details are given for the present data, but earlier data were obtained without charged track extrapolating to 1 cm of the shower center [7]. For UA6 and E706 (530), due to the difference in energy, these cuts cover about the same phase space while for WA70 the cut is more drastic. Cuts on the longitudinal energy deposition are implemented differently by WA70 (at the shower tail) and E706 (at the shower front) and are corrected for. These two kinds of cuts have more effects on bremsstrahlung than direct photon production, *i.e.* more effects at low p_T . Small differences on cross sections may result from the different cuts and the different ways their efficiencies are estimated. They are surely bounded by the expected size of the bremsstrahlung contribution (which should not exceed 20%).

5.3 Backgrounds

The experimental candidate photon samples are always contaminated by sizable backgrounds. With high granularity calorimeters such as those used by WA70, UA6 and E706, the backgrounds are mainly from π^0 . The amount of background depends on the calorimeter, for example granularity, and on the strategies adopted to reconstruct the showers. It obviously depends on p_T , on rapidity, and is important at low p_T in any case. The background corrections are performed with simulation of the known backgrounds in the detector, the simulation being checked on the reconstructed π^0 's.

Typical background fractions in the candidate photon sample are of order 50-60% at $p_T = 4.25$ GeV/c to 20-30% at $p_T = 5.5$ GeV/c (WA70, central rapidity); 70 to 80% at p_T of 4-5 GeV/c (E706 early data). For UA6 $\bar{p}p$ data, the corresponding figure is about 40% and depends on p_T while for pp it depends weakly on p_T and amounts to about 50% [38]. Typical uncertainties on the cross section quoted are 16% at $p_T = 4$ GeV down to 8% at p_T of 8 GeV/c for E706 early data. For WA70, the uncertainties were in the 10-25% range with an additional 15% upper limit from simulation. UA6 quotes specifically the various independent uncertainties on simulation in the 1 to 6% range.

Small errors on background evaluation induce large errors on the extracted signals. It is therefore very important to understand the background precisely. This point deserves further study as it may be helpful to understand discrepancies between experiments.

5.4 Comparison of data sets

Without theoretical prejudice, one can only compare data in a similar energy range. For the CERN fixed target data from the WA70 (beam of 280 GeV/c [3]) and the NA24 (beam of 300 GeV/c) experiments, “the agreement (at $y=0$) appears to be well within systematics and even statistical uncertainty” [39,40]. On the other hand, at ISR with $\sqrt{s} = 62.3$ GeV, “normalizations were about 1.5 to 2 in relative doubt” [39]¹.

Although most of the ISR prompt photon data have been taken at $\sqrt{s}=63$ GeV [2,5,6], data at lower \sqrt{s} ² are reported as γ/π^0 by the R806 collaboration (at $\sqrt{s} = 31$ GeV, 45 GeV and 63 GeV [2,42]). One can tentatively combine the data on γ/π^0 [42] at $\sqrt{s} = 31$ GeV with π^0 production cross sections (using the super-retracted data from Table 5 of [43] at $\sqrt{s} = 30.6$ GeV)³: the resulting γ cross sections turn out to be, within large experimental errors, compatible with the E706 results in the p_T range 4.0 – 6.0 GeV/c. It is worth mentioning that this is just a rough cross-check as the R806 collaboration did not publish a direct photon cross section at $\sqrt{s} = 31$ GeV⁴.

We have not included these data on the *data/theory* plots as they do not help to solve the observed discrepancies on these plots between the rough agreement with perturbative theory of the bulk of ISR data at low x_T and the strong disagreement of the E706 data at higher x_T : within the deduced experimental errors, these ratios for the data at $\sqrt{s} = 31$ GeV are compatible with the E706 data at $\sqrt{s} = 31.6$ GeV in the x_T range 0.26 – 0.39 but they are also compatible with 1. Unfortunately we therefore cannot conclude on ISR/E706 comparisons.

5.5 Summary on experimental data sets

Other effects, such as luminosity, trigger efficiencies, absolute energy scale, may affect the γ cross section. However they also affect the π^0 cross section. It is more relevant to discuss them in this context [45].

6 Conclusions

It appears that the present inclusive prompt photon data at various fixed target and ISR energies are incompatible:

¹ As for the published ISR data used in this present work, the discrepancy is in the slope in p_T rather than in the overall normalization

² Data on γ /all neutral clusters have been reported at $\sqrt{s} = 44.8$ GeV and 62.4 GeV by the R110 collaboration [41]. At fixed p_T , the γ /all neutral clusters decreases with \sqrt{s} [41] while γ/π^0 shows little \sqrt{s} dependence [2]

³ These π^0 cross sections are in fair agreement with measurements of the R110 collaborations at $\sqrt{s} = 31$ GeV [44]

⁴ As a check of this rough procedure, combining the same way data on γ/π^0 at $\sqrt{s} = 63$ GeV [42] with the super-retracted data at $\sqrt{s} = 62.8$ GeV of [43] one gets photon cross sections statistically compatible with [2]

normalizing the theory on one set, the extrapolation of the theory to a slightly different energy completely misses the corresponding data. Faced with these results, two alternatives are conceivable:

- Either one considers only the range over which perturbative QCD becomes reliable, *i.e.* p_T above 4 to 5 GeV/c depending on the center of mass energy. (For p_T below 4 or 5 GeV/c, the theory is unstable with respect to scale variations and one should not emphasize this kinematical region when comparing theory and data.) Then normalisation problems in the data prevent the standard QCD predictions to be in agreement with the experimental results.
- Or one emphasizes the whole p_T range and the standard QCD approach must be modified; this is the way adopted by the E706 and CTEQ collaborations who introduce a k_T effect. With an energy dependent k_T effect, these collaborations are able to obtain an overall agreement with some direct photon data while the agreement with other sets is destroyed.

This last option raises several questions on the physics of the k_T effect. An important one is the relation between the effect observed in single inclusive cross sections and in double inclusive cross sections. In perturbative QCD, they are not related. Non-perturbative effects might modify this statement; it is still an open question. In any case, an effort should be made by experimentalists to extend the discussion of Sect. 5 to better understand the various sources of systematic uncertainties. Perhaps RHIC, with a center-of-mass energy as low as 50 GeV, could help to resolve the important discrepancy observed between some data sets.

As a final remark, let us notice that all direct photon experiments also measure inclusive π^0 cross sections. It would be interesting to see whether the normalization discrepancies observed in direct photon experiments persist for the π^0 cross sections. Here the theoretical predictions are less reliable: 1) the cross sections depend on the fragmentation functions of quarks and gluons into π^0 ; 2) the effective value of the fragmentation variable z is in the range .8-.9 and large $\ln(1-z)$ terms should be resummed; 3) the scale dependence of the cross section is large. For all these reasons, we do not expect a very good agreement between data and theory in the p_T range of fixed target experiments [46]. We can however use the theoretical cross sections as reference curves and investigate how data are situated with respect to the predictions. Preliminary studies [45] show that fixed target data overshoot the theoretical curves by a few tens of percents, when CTEQ4M or MRST and the scales $p_T/3$ are used. Therefore all fixed target π^0 data display a similar behaviour compared to the theoretical cross sections and appear less scattered than the prompt photon data. This would indicate that the main problem rests with the extraction of the γ/π^0 ratio.

Acknowledgements. We thank L. Camilleri, J. Huston, G. Ginther and M. Zieliński for discussions.

References

1. E629 collaboration, M. McLaughlin et. al., Phys. Rev. Lett. **51** (1983) 971; NA3 collaboration, J. Badier et. al., Z. Phys. C **31** (1986) 341; NA24 collaboration, C. De Marzo et. al., Phys. Rev. D **36** (1987) 8; R108 collaboration, A.L.S. Angelis et. al., Nucl. Phys. B **263** (1986) 228; E704 collaboration, D. Adams et al., Phys. Lett. B **345** (1995) 569
2. R806 collaboration, E. Annassontzis et. al., Z. Phys. C **13** (1982) 277
3. WA70 collaboration, M. Bonesini et al., Z. Phys. C **37** (1988) 535
4. WA70 collaboration, M. Bonesini et al., Z. Phys. C **38** (1988) 371
5. R110 collaboration, A.L.S. Angelis et. al., Nucl. Phys. B **327** (1989) 541
6. AFS/R807 collaboration, T. Åkesson et. al., Sov. J. Nuc. Phys. **51** (1990) 836
7. E706 collaboration, G. Alverson et al., Phys. Rev. D **48** (1993) 5
8. E706 collaboration, L. Apanasevich et al., Phys. Rev. Lett. **81** (1998) 2642
9. UA6 collaboration, G. Balocchi et al., Phys. Lett. B **436** (1998) 222
10. For a compilation of data, see W. Vogelsang, M.R. Whalley, J. Phys. G **23**, Sup. 7A (1997) A1
11. H. Fritzsch, P. Minkowski, Phys. Lett. **71B** (1977) 392
12. P. Aurenche, R. Baier, M. Fontannaz, D.Schiff, Nucl. Phys. B **297** (1988) 661
13. P. Aurenche, P. Chiappetta, M. Fontannaz, J.Ph. Guillet, E. Pilon, Nucl. Phys. B **399** (1993) 34
14. L.E. Gordon, W. Vogelsang, Phys. Rev. D **50** (1994) 1901
15. G. Grunberg, Phys. Rev. D **29** (1984) 2315
16. P.M. Stevenson, Phys. Rev. D **23** (1981) 2916; P.M. Stevenson, H.D. Politzer, Nucl. Phys. **277** (1986) 758
17. S.J. Brodsky, G.P. Lepage, P.B. Mackenzie, Phys. Rev. D **28** (1983) 228
18. P. Aurenche, R. Baier, M. Fontannaz, D. Schiff, Nucl. Phys. B **286** (1987) 509
19. P. Aurenche, R. Baier, M. Fontannaz, J.F. Owens, M. Werlen, Phys. Rev. D **39** (1989) 3275
20. W. Vogelsang, A. Vogt, Nucl. Phys. B **453** (1995) 334
21. L.E. Gordon, Nucl. Phys. B **501** (1997) 175
22. J. Huston, E. Kovacs, S. Kuhlmann, H.L. Lai, J.F. Owens, W.K. Tung, Phys. Rev. D **51** (1995) 6139
23. T. Ferbel, in proceedings of the 1996 Rencontres de Moriond, hadronic session, J. Trân Thanh Vân ed., Editions Frontières
24. L. Apanasevich et al., Phys. Rev. D **59**: 074007 (1999)
25. M. Zielinski, hep-ph/9811278
26. F. Aversa, P. Chiappetta, M. Greco, J.Ph. Guillet, Nucl. Phys. B **327** (1989) 105
27. CTEQ collaboration, H.L. Lai et al., Phys. Rev. D **55** (1997) 1280
28. A.D. Martin, R.G. Roberts, W.J. Stirling, R.S. Thorne, Eur. Phys. J. Eur. Phys. J. C **4** (1998) 463
29. M. Glück, E. Reya, A. Vogt, Eur. Phys. J. C **5** (1998) 461
30. M. Glück, E. Reya, A. Vogt, Phys. Rev. D **48** (1993) 116; Erratum: ibid. D **51**,1427
31. L. Bourhis, M. Fontannaz, J.Ph. Guillet, Eur. Phys. J. C **2** (1998) 529
32. E. Laenen, G. Oderda, G. Sterman, Phys. Lett. B **438** (1999) 173; S. Catani, M.L. Mangano, P. Nason, J. High Energy Phys. (1998) 9807:024
33. M. Fontannaz, D. Schiff, Nucl. Phys. B **132** (1978) 457
34. M. Fontannaz in proceedings of the 1997 Rencontres de Moriond, hadronic session, J. Trân Thanh Vân ed., Editions Frontières
35. UA6 collaboration, G. Balocchi et al., Phys. Lett. B **317** (1993) 250; M. Werlen in Proc. Int. Europhysics Conf. on High Energy Physics, EPS 93, Marseille, ed. by J. Carr, M. Perrottet, (Editions Frontières) 323; UA6 Collaboration, M. Werlen et al., CERN-EP/99-021
36. U.K. Yang, A. Bodek, Q. Fan, in proceedings of the 1998 Rencontres de Moriond, hadronic session, J. Trân Thanh Vân ed., Editions Frontières
37. E706 collaboration, private correspondence
38. see Ph. D. theses D. Hubbard (Michigan 1993), P. Oberson (Lausanne 1994), C. Comtat (Lausanne 1996), N.M. Chung (Lausanne 1998)
39. T. Ferbel in Proc. Physics in Collisions, Capri 1988, 255, P. Strolin ed., Editions Frontières
40. M. Martin in Proc. QCD Workshop, St. Croix 1988, B. Cox ed., Plenum Pub. Corp.
41. R110 collaboration, A.L.S. Angelis et al., Phys. Lett. **98B** (1981) 115
42. R806 collaboration, M. Diakonou et al., Phys. Lett. **91B** (1980) 296
43. R806 collaboration, C. Kourkoumelis et al., Z. Phys. C **5** (1980) 95
44. R110 collaboration, A.L.S. Angelis et al., Phys. Lett. **185B** (1987) 213
45. P. Aurenche, M. Fontannaz, J.Ph. Guillet, B. Kniehl, E. Pilon, M. Werlen, preprint in preparation
46. P. Chiappetta, M. Greco, J.Ph. Guillet, S. Rolli, M. Werlen, Nucl. Phys. B **412** (1994) 3